Low Latitude Ionospheric D-region Dependence on Solar Zenith Angle

Neil R. Thomson,[1] Mark A. Clilverd[2] and Craig J. Rodger[1]

[1]Physics Department, University of Otago, Dunedin, New Zealand.

[2]British Antarctic Survey, Cambridge, UK.

Abstract: Phase and amplitude measurements of VLF radio signals on a short, nearly all-sea path between two Hawaiian Islands are used to find the height and sharpness of the lower edge of the daytime tropical D-region as a function of solar zenith angle (SZA). The path used was from US Navy transmitter NPM (21.4 kHz) on Oahu to Keauhou, 306 km away, on the west coast of the Big Island of Hawaii, where ionospheric sensitivity was high due to the destructive interference between the ionospherically reflected wave and the ground wave, particularly around the middle of the day. The height and sharpness are thus found to vary from $H' = 69.3 \pm 0.3$ km and $\beta = 0.49 \pm 0.02$ km^{-1} for SZA ~10°, at midday, to $H' > 80$ km and $\beta \sim 0.30$ km^{-1} as the SZA approached ~70°-90°, near dawn and dusk for this tropical path. Additional values for the variations of H' and β with solar zenith angle are also found from VLF phase and amplitude observations on other similar paths: the short path NWC to Karratha (in N.W. Australia), and the long paths, NWC to Kyoto in Japan, and NAU, Puerto Rico, to St. John's Canada. Significant differences in the SZA variations of H' and β were found between low and mid-latitudes resulting from the latitudinally varying interplay between Lyman-α and galactic cosmic rays in forming the lower D-region. Both latitude ranges showed $\beta < 0.30$ km^{-1} during sunrise/sunset conditions.

1. Introduction

The lowest altitude part of the Earth's ionosphere is the lower D-region for which, at least from its effects on very low frequency (VLF: ~3-30 kHz) radio waves, the electron number density**, *N(z)* in m^{-3}, versus height, *z* in km, has been found to be conveniently described (e.g. in the US Navy VLF waveguide codes, ModeFinder and LWPC) by the two Wait parameters, the height, *H'* in km, and the sharpness, β in km^{-1} as:**

$$N(z) = 1.43 \times 10^{13} \exp(-0.15H') \exp[(\beta - 0.15)(z - H')]$$

[*Wait and Spies,* 1964; *Morfitt and Shellman,* 1976; or e.g. *Thomson,* 1993]. The sharpness parameter, β, is thus a measure of how rapidly the electron density is increasing with height. This modeling of the electron density increasing exponentially with height in the lower D-region (~50-80 km altitude) is, of course, an approximation. However, experimental rocket profiles such as those of *Mechtly et al.* [1972] plus the rocket profiles and modeling of *Friedrich and Torkar* [1998] provide independent evidence that this is a reasonable approximation to reality. D-region modeling, particularly for the loss processes, is not yet sufficiently advanced to offer workable alternative profiles, and so most successful modeling of the lower D-region, at least for VLF propagation, continues to use these simple two parameter (*H'*, β) profiles.

When the Sun is nearly overhead at midday, *H'* is ~70 km and β ~0.45-0.5 km^{-1}. By day, the upper part of the lower D-region is ionized mainly by Lyman-α from the Sun while the lower part (below 65-70 km) is principally ionized by galactic cosmic rays [e.g., *Banks and Kockarts*, 1973]. The cosmic rays are omnidirectional so their ionizing effects are not affected by time of day and solar zenith angle. In contrast, when the Sun is lower in the sky (i.e., has a greater solar zenith angle, SZA), the Lyman-α from the Sun passes through the Earth's atmosphere at more oblique angles undergoing more atmospheric absorption, and so produces less ionization at a given altitude than for the Sun high in the sky. This reduced ionization in the upper part of the lower D-region, while the Sun is lower in the sky near dawn and dusk, results in the sharpness, β, being smaller nearer dawn and dusk compared with midday [*Thomson and Clilverd*, 2001].

Although the cosmic ray intensity in the D-region does not vary with time of day, the intensity does vary significantly with geomagnetic latitude, being markedly higher in polar-regions than near the equator because of the shielding effect of the Earth's magnetic field at low latitudes [e.g. *Heaps*, 1978]. This means that the dependence on solar zenith angle of the D-region electron density parameters can be expected to show some latitude dependence. Understanding the interplay between the effects of Lyman-α and galactic cosmic rays is key to improving long-wave propagation codes, which in turn will enhance the usefulness of the codes to applications like the AARDDVARK network of Space Weather monitors [*Clilverd et al*., 2009].

When the Sun's altitude lowers towards dawn or dusk, *H'* rises to well above 75 km, and β falls to ~0.30 km^{-1} or lower [*Thomson,* 1993, *McRae and Thomson,* 2000]. In these two previous studies the dependence of *H'* and β on time of day, and hence solar zenith angle, depended on observations on long paths which had both mid-latitude and low latitude components, and for which the solar zenith angle also typically varied appreciably along the path, particularly near dawn and dusk. *Han and Cummer* [2010] and *Han et al.* [2011] used natural lightning to determine values for *H'* and β as functions of solar zenith angle but at a significantly higher latitude (magnetic dip ~47° N) than the low latitudes studied here. Here we use VLF amplitude and phase measurements on a low-latitude, short, nearly all-sea path between two Hawaiian Islands: from NPM (21.4 kHz) on Oahu to the Big Island of Hawaii. The whole of the path is within ~1° of 20.5° N geographic which is also within ~1° of magnetic dip latitude 20.5° N at this longitude. These experimental observations are then compared with modeling calculations to determine values for the ionospheric parameters, *H'* and β, both at midday and also as functions of solar zenith angle.

Results from this Hawaiian path are then compared with those from another short path, NWC (19.8 kHz) to Karratha (N.W. Australia) [*Thomson*, 2010; *Thomson et al*., 2011b and 2012], mainly over the sea, which has a similarly tropical geographic latitude, ~21° S, but has a somewhat higher (though still low) magnetic dip latitude, ~36° S. Further comparisons of the dependence of H' and β on solar zenith angle are then made using the trans-equatorial, nearly all-sea, low-latitude path, NWC to Kyoto, Japan, and for the low- to mid-latitude, nearly all-sea path NAU (40.75 kHz) on Puerto Rico to St John's, Canada, using VLF phase and amplitude recordings over several days in both cases.

2. VLF Measurement Techniques

2.1 The Portable VLF Loop Antenna and Receiver

The phases and amplitudes of the VLF signals in Hawaii and N.W. Australia were measured with a GPS-referenced portable loop receiver, details of which are given in *Thomson* [2010]. These measurements were taken at sites well away from (buried/overhead) conductors such as power lines, checking for self-consistency over horizontal distances of at least a few tens of meters and from one (nearby) site to the next. The portable loop system measures the phases as delays in μs with respect to the GPS 1-s pulses. These delays are modulo half-a-period of the VLF frequency [*Thomson*, 2010].

2.2 The Fixed VLF Recorders near Seattle WA USA

A fixed, GPS-referenced, 'UltraMSK' receiver recorded the phases and amplitudes of US Navy transmitter, NPM, at Forks on the Olympic peninsula near Seattle WA USA while the portable loop measurements were being made in Hawaii. This enabled correcting for phase drifts and for weekly (or sometimes more frequent) phase jumps at the transmitters, because the daytime propagation for this 4.2 Mm NPM-Seattle path is very stable, especially in summer. The Forks site is part of the Antarctic-Arctic Radiation-belt Dynamic Deposition VLF Atmospheric Research Konsortia (AARDDVARK) network [*Clilverd et al.*, 2009]; further information and a description of the array can be found at www.physics.otago.ac.nz/space/AARDDVARK_homepage.htm.

3. VLF Measurements and Modeling Comparisons

3.1 The Short Path NPM to the Big Island of Hawaii

The 306-km, nearly all-sea path from NPM (21.4 kHz) on Oahu to Keauhou on the Big Island of Hawaii, used here to determine lower D-region ionospheric parameters, is shown in Figure 1. Also shown in Figure 1 is the very short (140-km) path from NPM to Kauai used to determine the phase at the NPM transmitter because, for a path this short, the received signal comes mainly from the (readily calculated) ground wave with only a minor contribution from the ionosphere. Similarly, this very short path also enables a check on the radiated power of NPM, largely independent of any ionospheric influence.

NPM amplitudes and phases were measured with the portable loop system near Keauhou 19-25 Aug 2012 LT (LT = HAST = UT - 10) and on Kauai 26 Aug – 31 Aug 2012 LT, except when NPM was scheduled to be off-air for its weekly maintenance (late on 22 and 29 Aug UT). Several days of the phase and amplitude measurements made with the UltraMSK recorder at Forks WA near Seattle, while the Hawaiian measurements were being made, are shown in Figure 2. The general stability of the amplitude is an indication of the stability of the propagation path from NPM to Seattle in summer and hence the usefulness of the Seattle recordings in monitoring the transmitter's amplitude and phase. For the period 23-28 Aug 2012 shown in Figure 2, NPM had a moderate frequency offset from its nominal 21.4 kHz. To allow the phase to be plotted in a range of less than ~100°, and so give an indication of phase stability, an offset of 34.5° per hour has been removed from the recorded GPS-referenced phase at 21.4 kHz.

3.2 Short Path ModeFinder Calculations Compared with Observations

A slightly modified version of the US Navy waveguide code, ModeFinder [*Morfitt and Shellman*, 1976], was used to calculate phases and amplitudes of NPM (21.4 kHz) at Keauhou 306 km away on the 'Big Island' of Hawaii for a range of values for the ionospheric D-region parameters, height *H'* in km, and sharpness β in km^{-1}. The technique used here is the same as that used for the ~300-km path NWC to Karratha reported by *Thomson* [2010]. As previously, ModeFinder was set to calculate B_y, the horizontal component of the magnetic field of the wave (rather than the more usual vertical electric field, E_z) because the portable loop antenna, used here for the observations, effectively measures B_y. None-the-less, all the amplitudes presented here are expressed in V/m (using $E_z = cB_y$), typically as dB > 1 μV/m, as is common for specifying VLF amplitudes. Figure 3 shows the results of the ModeFinder calculations and also, as a solid straight line, the observed average midday amplitude of NPM measured at Keauhou, 74.4 dB > 1 μV/m. The radiated power for NPM was again taken as 375 kW as determined from amplitude measurements on Kauai (~140 km WNW of NPM) both previously [*Thomson et al*., 2011b, 2012] and during the period 26-31 August 2012, shortly after the Keauhou measurements presented here.

More than 30 sets of phase and amplitude measurements for NPM were taken with the GPS-referenced portable loop receiver within 1-2 hours of local midday on Kauai, mainly at sites in Lydgate Park (on the east coast), 140 km from NPM, on the 5 days 26-28, 30-31 August 2012. As previously [*Thomson et al.*, 2011b, 2012], the signal strength of NPM on Kauai required reducing the gain of the portable loop system by having two 750 Ω resistors in series with the loop rather than the usual two 39 Ω resistors as mainly used at Keauhou. After adjusting the Lydgate Park, Kauai, phase readings from 2 × 750 Ω to 2 × 39 Ω, it was found that 17.9 μs phase delay at Lydgate corresponded to -6° on the UltraMSK recorder at Seattle during the 6-day period of the Lydgate readings.

Many portable loop phase and amplitude measurements of NPM were made at Keauhou on the Big Island of Hawaii, ~306 km from NPM, during the period 19-25 August 2012. This location was near a midday modal minimum where the ground wave was ~20 mV/m and the ionospherically reflected (or ‘sky’) wave was ~15 mV/m giving a resultant amplitude ~5 mV/m, resulting in a relatively high sensitivity to the ionospheric conditions. The latitudes and longitudes for NPM and for the principal Keauhou and Lydgate sites are shown in Table 1 which also shows the great-circle distances, NPM-Lydgate and NPM-Keauhou, calculated using the Vincenty algorithm [*Vincenty,* 1975] and the corresponding free-space delays in μs calculated from these distances using the (exact) speed of light.

The phase delays in μs measured at Keauhou (relative to GPS 1-pps) need to be appropriately adjusted in time, and converted to degrees, for direct comparison with the output, in degrees, of ModeFinder calculations for NPM-Keauhou. The resulting observed phases at Keauhou in 'ModeFinder degrees' are shown as functions of time in Figure 4 in the upper panel. This conversion of phase delay to 'ModeFinder' degrees at Keauhou can be conveniently illustrated using the following example. At 2309 UT on 21 August 2012, the phase delay measured at Keauhou was 25.2 μs while the phase on the recorder at Seattle was -120.5° ≡ 59.5° (modulo 180°). As mentioned earlier, 17.9 μs at Lydgate corresponded to -6° at Seattle, so the observed time delay difference for NPM-Keauhou and NPM-Lydgate was

$$25.2 – 17.9 + [59.5 - (-6)]/360/0.0214 = 15.8 \ \mu s.$$

This observed time delay difference effectively consists of two parts: (1) the free space delay and (2) the waveguide-only part of the delay that ModeFinder (and other codes such as LWPC) calculate. From the Vincenty great circle calculations shown in Table 1, the free space part of the delay difference (modulo half-a-period) is 14.3 μs so the waveguide-only part of the delay difference is 15.8 - 14.3 = 1.5 μs which is equivalent to 11.5° at 21.4 kHz. ModeFinder calculates the phase at Lydgate as 40.5°. Hence the Keauhou observed phase in 'ModeFinder degrees' (for this example data point at 2309 UT on 21 August 2012) is 40.5 – 11.5 = 29° as shown in Figure 4. The phase of 40.5° which ModeFinder calculated for NPM-Lydgate was for H' = 69.3 km and β = 0.49 km^{-1}, the midday parameters found from the Keauhou measurements. The phase at Lydgate is however, not very sensitive to the ionospheric parameters because the signal at Lydgate is mainly ground wave, partly because Lydgate is closer to NPM than Keauhou (140 km versus 306 km) and partly because west-to-east ionospheric reflection, such as for NPM-Keauhou, is much less attenuating than east-to-west reflection, such as for NPM-Lydgate, particularly at such low latitudes.

From Figure 4 it can be seen that, at midday, the mean observed phase of NPM at Keauhou, averaged over all the measurement days, was 30° (in 'ModeFinder degrees'); this average is shown as a solid straight line in the top panel of Figure 3 to allow comparison with the ModeFinder calculations. Similarly the midday average observed amplitude of NPM at Keauhou from Figure 4 was 74.4 dB > 1 μV/m and this is also shown as a solid straight line in the appropriate panel of Figure 3. Thus from Figure 3 it can be seen that the midday ionospheric D-region observations at latitude ~20° N (both geographic and magnetic dip) for the 306 km path NPM to Keauhou can be best represented by $H' = 69.3 \pm 0.3$ km and $\beta = 0.49 \pm 0.02$ km^{-1}.

Similarly, the observed values of phase in degrees and amplitude in dB at times other than midday from Figure 4 were also used in the ModeFinder plots of Figure 3 (shown there as the larger open circles) to determine appropriate values of H' and β over a range of times of day and hence solar zenith angles. The H' and β values so determined are plotted in Figure 5, where the solar zenith angles are shown as negative in the morning and positive in the afternoon. Also shown in these H' and β plots in Figure 5, for comparison, are a similar set of results from the 300-km path NWC (19.8 kHz) to Karratha in N.W. Australia over 5 days in mid-October 2011. The path NWC-Karratha, being at ~21° S., geographic, is at a very similar distance from the equator to the NPM-Keauhou path. In both cases the measurements were made about a month on the summer side of the September equinox (August for NPM-Keauhou and October for NWC-Karratha) and so the Sun was ~10° from the zenith at midday in both cases. Although both paths are nearly all-sea, the NWC-Karratha path is potentially more affected by land, partly because more of the path, albeit mainly close to the sea, is over land, and partly because the land has lower conductivity, ~0.001 S/m as compared with ~0.01 S/m in Hawaii, according to the Westinghouse conductivity estimates used in the US Navy's LWPC VLF propagation code.

In Figure 5, it can also be seen that β falls only to ~0.37 km^{-1} near dawn and dusk (i.e., at solar zenith angles around 70°-80°) for the NWC-Karratha path but falls to ~0.30 km^{-1} for the NPM-Keauhou path. By comparing with results from other longer paths (considered later), it appears that the anomaly lies with the NWC-Karratha path and is likely due to a combination of several factors. The first, as mentioned above, is the low (and so likely uncertain and variable) conductivity of the ground at the Karratha receiver site. The second is the higher magnetic dip latitude of the NWC-Karratha path (~36°) compared with the NPM-Keauhou path (~20°). While there is ample ionospherically reflected ('sky') wave for both these west-to-east paths near midday, the higher magnetic dip latitude for NWC-Karratha significantly reduces the otherwise enhanced low latitude reflections for west-to-east propagation particularly at the lower values of β near dawn and dusk. The wave hop code of *Berry and Herman* [1971] shows that for H' = 79 km and β = 0.3 km^{-1} (i.e, solar zenith angles ~75°-80°) the 'sky' wave amplitude is ~30% of the ground wave at Keauhou but only ~17% at Karratha, principally due to the higher magnetic dip latitude for NWC-Karratha. A further possibly complicating factor for Karratha was that, while the measurements near midday were made outdoors at good sites, the measurements for solar zenith angles more than 30°- 40° (nearer dawn and dusk) were mainly made indoors. Although significant efforts were made to calibrate the indoor site with respect to the outdoor sites, some uncertainty must remain. A very small number of dawn-dusk readings in Karratha made in August 2011 (in contrast to the main set in October 2011) were made at a good outdoor site; these suggested that β dropped to ~0.33 km^{-1} (as compared with the ~0.37 km^{-1} found indoors in October). In contrast, all the NPM-Keahou measurements were made outside at what appeared to be reliable sites. However, as can be seen in Figure 5, even for NPM-Keauhou, β did not drop much below ~0.30 km^{-1} just after dawn or just before dusk.

To indicate the extent of any am/pm (morning/afternoon) asymmetries about mid-day, the observed pm (afternoon) values of H' and β (black lines and black squares), after being reflected about mid-day for NPM-Hawaii, are also shown in Figure 5 as blue crosses and blue

dotted lines. It can thus be seen that *H’* is generally slightly lower, and *β* is slightly higher, in the afternoon than in the morning for a given solar zenith angle, indicating a slight ‘sluggishness’ in the development of the lower D-region during the day. For the NWC-Karratha path, the effect is similar for *H’* but smaller or non-existent for *β*. (For the longer VLF paths discussed later the angles between path and the terminator are too different between morning and afternoon to meaningfully test for this relatively small effect.)

In view of the possible uncertainties near dawn and dusk, mainly for *β*, due to the relatively low proportion of ‘sky’ wave relative to the direct ground wave on short paths (particularly NWC-Karratha), it seemed desirable to check the *β* (and *H’*) variations with solar zenith angle on longer, preferably otherwise similar, low-latitude paths where the ionospherically reflected (‘sky’) wave dominates at the receiver. This is done in the next two sub-sections below.

3.3 Comparison with Observations on the Trans-equatorial Path NWC to Kyoto

Araki et al. [1969] measured and reported averaged diurnal phase and amplitude variations with time of day for NWC in Kyoto, Japan, at solar maximum, on both 15.5 kHz (31 July – 7 August 1968) and 22.3 kHz (7-14 August 1968). This 6.7-Mm path is nearly all-sea and mainly at low magnetic dip latitudes, going from dip latitude ~36° S at NWC across the equator to Uji in Kyoto (34° 54’ N, 135° 48’ E) at dip latitude ~29° N. These observed phases and amplitudes are now compared with calculated phases and amplitudes obtained using a slightly modified version of the US Navy subionospheric VLF code LWPC [*Ferguson and Snyder*, 1990] which calculates E_z using very similar modal techniques to ModeFinder but is preferred for longer paths because it automatically allows for the variations in the Earth’s magnetic field which occur along such paths. (The ability of ModeFinder to calculate B_y rather than E_z is not needed on such long paths because the differences between using B_y rather than E_z on long paths is negligible.)

While the phase observations of *Araki et al.* [1969] give the changes in phase of NWC at Kyoto with time of day and hence solar zenith angle, these phases are relative rather than absolute because no phases were measured near the transmitter. Similarly, their results reliably give the diurnal changes in amplitude at Kyoto but there is uncertainty about the power NWC was radiating in August 1968 (shortly after it was commissioned) and also about the absolute level of the amplitudes at the receiver. However, these issues were satisfactorily resolved here by using appropriate midday (solar maximum) values of *H'* and β for this path derived from the results reported here and in *Thomson et al.* [2011a, 2011b and 2012]. The (average) values so adopted for the midday NWC to Kyoto path in August 1968 were *H'* = 70.1 km and β = 0.48 km^{-1}, after allowing for the small but non-negligible variations in solar zenith angle along the path at midday.

The resulting observed diurnal variations of *H'* and β with solar zenith angle from the NWC-Kyoto path, for both 15.5 kHz and 22.3 kHz, are shown in Figure 6 where the agreement with the NPM-Keauhou short path results can be seen to be generally good. However, for the long NWC-Kyoto path, β clearly drops to well below 0.30 km^{-1} when the Sun is just above the horizon near dawn and dusk. For this long path the signal at the receiver is virtually all ionospherically reflected – the ground wave part at Kyoto is very small due to the Earth's curvature. In contrast, for the short paths near dawn and dusk, the amplitude of the ionospherically reflected signal at the receiver, as mentioned previously, is relatively small compared with that of the ground wave particularly for the NWC-Karratha path. This implies that the long path is probably giving the correct ionospheric attenuation and so the correct value for the ionospheric sharpness, β, near dawn and dusk. However, it might also be possible, that the D-region very near the magnetic dip equator (i.e., closer to the dip equator than the NPM-Keauhou path) has even lower values of β near dawn and dusk which do not extend to magnetic dip latitudes of 20° or higher. This is tested below by examining results from a low to mid-latitude VLF path which does not go closer to the magnetic dip equator than 20°.

3.4 Comparison with Observations on the Non-equatorial Path NAU, Puerto Rico, to St. John's, Canada

US Navy transmitter, NAU, on the Caribbean island of Puerto Rico radiates ~100 kW on 40.75 kHz. Like other US Navy VLF transmitters it uses 200-baud MSK modulation. Its location is ~18.4° N, 67.2° W geographic which corresponds to a magnetic dip latitude of ~26°. At St. John's NL, Canada, 47.6° N, 52.7° W, dip latitude ~50° and 3500 km away, over a very nearly all-sea path, the British Antarctic Survey AARDDVARK receiver continuously records the amplitudes and phases of several VLF transmitters, including NAU, with a high time resolution. To find *H'* and β from these phases and amplitudes, comparisons from the recordings in the period 11-18 June 2013 were made using the wave hop subionospheric VLF code of *Berry and Herman* [1971] rather than LWPC because LWPC is rated only up to 30 kHz while their wave hop code is designed to go up to 60 kHz. **Recently *Yoshida et al.* [2008] also used a wave hop code for subionospheric propagation at frequencies of ~40 kHz.** As for the NWC-Kyoto path, the output power of the transmitter (NAU) was somewhat uncertain. While the recorder at St. John's is GPS-referenced, the phase at the NAU transmitter relative to GPS 1-s pulses was unknown. However, as for the NWC-Kyoto path, *H'* and β at midday could be estimated fairly well from previous measurements at low and middle latitudes near solar maximum, taking into account known variations of midday *H'* and β with latitude, in particular, for NAU-St. John's, decreases in β with increasing magnetic latitude due to the corresponding galactic cosmic ray intensity increases [*Thomson et al.*, 2011a, 2011b, 2012].

The (average) values so adopted for the midday NAU to St. John's path in June 2013 were *H'* = 70.5 km and β = 0.43 km^{-1}, after making allowance for the expected variations in *H'* and β along the path at midday due to changes in latitude and solar zenith angle (from near overhead at the tropical end of the path to ~25° at St. John's). Using very similar procedures to those used for Figure 6, Figure

7 shows H' and β, averaged along the NAU-St. John's path, as functions of solar zenith angle. Again, as can be seen, it is clear that, at these higher latitudes too, β falls below 0.30 km^{-1} for high daytime solar zenith angles. For this path, the receiver at St. John's is not directly north of NAU but somewhat to the east of north. This means that, at this time of year (June) the sunset terminator is nearly aligned with the path so all parts of the path have similar solar zenith angles in the afternoon-dusk period, making this period very suitable for comparisons.

However, in the dawn-morning period the sunrise terminator is not well aligned with the path and so the solar zenith angles vary considerably along the path. In particular, even 1 hour after sunrise at the path mid-point, the Sun was still below the horizon at NAU making it difficult to have meaningful averages along the path at such times. Thus the morning 'outlier' points in the -90° to -70° degree range for NAU-St. John's (shown in Figure 7 as black diamonds) are likely of limited value here.

4. Discussion, Summary and Conclusions

4.1 Midday H' and β at Low Latitudes

The midday measurements reported here in s3.2 for the 306 km Hawaiian path NPM-Keauhou give H' = 69.3 ± 0.3 km and β = 0.49 ± 0.02 km^{-1} for the lower edge of the ionospheric D-region at 20° N (both geographic and magnetic dip latitude) in August 2012, near the current (weak) solar maximum. The most comparable tropical D-region results available are those from the 300-km NWC-Karratha and NWC-Dampier paths where, for midday in October 2011, *Thomson et al.* [2012] found H' = 69.65 ± 0.5 km and β = 0.49 ± 0.03 km^{-1}. Additional measurements at midday on the NWC-Karratha path in late September 2012 gave H' = 69.8 ± 0.5 km and β = 0.46 ± 0.03 km^{-1}. After allowing for the slightly lower solar zenith angle for NWC-Karratha in September, reasonable estimates for the NWC-Karratha path for October 2011/2012 are H' = 69.7 ± 0.4 km and β = 0.48 ± 0.03 km^{-1}. At Karratha, October is one month on the summer side of equinox while in Hawaii August (when the measurements were made) is also one month on the summer side of equinox. The midday value of β found at Karratha (0.48 km^{-1}) is thus very comparable with that found for Hawaii (0.49 km^{-1}) particularly as Karratha has the higher, though still fairly low, magnetic dip latitude (~36° for NWC-Karratha, 20° for NPM-Keauhou), and so a slightly lower value of β is to be expected there. This midday value of H' = 69.7 ± 0.4 km at Karratha is somewhat higher than the value of H' = 69.3 ± 0.3 km found here for Hawaii. Clearly the difference might be just within the estimated experimental errors. However, *Thomson et al.* [2011b] used the neutral atmosphere MSIS-E-90 model to find the expected changes in H' with latitude and season. These results show that H' would be expected to be lower in August at ~20° N (Hawaiian latitudes) by ~0.3 km in comparison with ~21° S in October (NWC-Karratha latitudes). Thus the midday agreement in H' between the Hawaiian and N.W. Australian measurements appears to be as good as ~0.1 ± 0.3 km.

4.2 Changes in H' and β with Daytime Solar Zenith Angle

Phase and amplitude measurements for the short, virtually all-sea, NPM-Keauhou path in Hawaii were made over a wide range of daytime solar zenith angles and compared with ModeFinder calculations resulting in determining how H' and β vary with solar zenith angle at much lower latitudes (20° N, geographic and magnetic dip) than previously determined. These results were then compared with those from the short NWC-Karratha path near the coast of N.W. Australia at a similar geographic latitude (~21° S) but slightly higher magnetic dip latitude (~36°). While the agreement between the two sets of measurements was generally reasonable, it was noted that for the NWC-Karratha path, as the solar zenith angle increased towards dawn and dusk, β fell only to ~0.37 km^{-1} whereas for the lower latitude, all-sea, Hawaiian path it fell to ~0.30 km^{-1}. This was tentatively attributed mainly to a combination of the much lower proportion of ionospherically reflected signals at the higher magnetic dip latitudes near Karratha and the influence of the low conductivity ground on part of the NWC-Karratha path.

To check whether the low ground conductivity and the low proportion of ionospherically reflected wave at the receiver were likely to be the cause of these anomalously high values of β at high solar zenith angles for the NWC-Karratha path, diurnal phase and amplitude changes from the long, mainly low latitude, transequatorial, nearly all-sea path, NWC-Kyoto, were compared with calculations. The resulting H' and β changes with solar zenith angle for this long path agreed well with the short path results except that the long-path β clearly went well below 0.30 km^{-1}. For this long path the amplitude of any ground wave at the receiver is negligible; virtually all of the signal at the receiver is ionospherically reflected 'sky' wave. These long path results thus strongly support the ionospheric sharpness, β, going below 0.30 km^{-1} towards dawn and dusk.

However, as mentioned in s3.3 above, there remained the possibility that β goes below 0.30 km^{-1} only for magnetic dip latitudes below ~20°. Much of the transequatorial, NWC-Kyoto path would thus have low β and hence high attenuation (near dawn and dusk) so that the whole path would necessarily show low β and high attenuation as observed. To test if β also goes below 0.30 km^{-1} for somewhat higher latitudes, phase and amplitude changes recorded on the long, 3.5-Mm, NAU-St. John's path were also compared with calculations. Again β was found to go well below 0.30 km^{-1} for this path, which spans a dip latitude range ~26-50°. It is thus clear that the ionospheric sharpness, β, does go well below 0.30 km^{-1} near dawn and dusk at least from equatorial latitudes to low mid-latitudes.

Acknowledgements

The authors are very grateful to David Hardisty for his design, development and construction of the portable VLF phase meter. The recorded data used in Figures 2 and 7 are available on British Antarctic Survey web site, http://psddb.nerc-bas.ac.uk. The data measurements underlying Figures 3 and 5 are available from author N.R.T., while those for Figure 6 come from *Araki et al.* [1969].

References

Araki, T., S. Kitayama, and S. Kato (1969), Transequatorial reception of VLF radio waves from Australia, *Radio Sci.*, *4*(4), 367-369.

Banks, P. M., and G. Kockarts (1973), *Aeronomy*, Academic, New York.

Berry, L.A. and J.E. Herman (1971), *A wave hop propagation program for an anisotropic ionosphere,* OT/ITS Research Rep. 11, U.S. Dept. of Commerce, Boulder, Colo.

Clilverd, M. A., C. J. Rodger, N. R. Thomson, J. B. Brundell, Th. Ulich, J. Lichtenberger, N. Cobbett, A. B. Collier, F. W. Menk, A. Seppälä, P. T. Verronen, and E. Turunen (2009), Remote sensing space weather events: the AARDDVARK network, Space Weather, 7, S04001, doi:10.1029/2008SW000412.

Ferguson, J. A. and F. P. Snyder (1990), Computer programs for assessment of long wavelength radio communications, version 1.0: Full FORTRAN code user's guide, *Naval Ocean Systems Center Tech. Doc. 1773, DTIC AD-B144 839*, Def. Tech. Inf. Cent., Alexandria, Va.

Friedrich, M., and K.M. Torkar (1998), Empirical D-region modelling, a progress report, *Adv. Space Res.*, 22(6), 757-766.

Han F., and S.A. Cummer (2010), Midlatitude daytime D region ionosphere variations measured from radio atmospherics, *J. Geophys. Res.*, *115*, A10314, doi:10.1029/2010JA015715.

Han F., S.A. Cummer, J. Li, and G. Lu (2011), Daytime ionospheric *D* region sharpness derived from VLF radio atmospherics, *J. Geophys. Res.*, *116*, A05314, doi:10.1029/2010JA016299.

Heaps, M.G. (1978), Parameterization of the cosmic ray ion-pair production rate above 18 km. *Planet. Space Sci.*, 26, 513-517.

McRae, W. M. and N. R. Thomson (2000), VLF phase and amplitude: daytime ionospheric parameters, *J. Atmos. Sol.-Terr. Phys.,* 62(7), 609-618.

Mechtly, E.A., S.A. Bowhill, and L.G. Smith (1972), Changes of lower ionosphere electron concentrations with solar activity, *J. Atmos. & Terr. Phys.*, 34(11), 1899-1907.

Morfitt, D. G. and C. H. Shellman (1976), MODESRCH, an improved computer program for obtaining ELF/VLF/LF mode constants in an Earth-Ionosphere Waveguide. *Naval Electr. Lab. Cent. Interim Rep. 77T, NTIS Accession ADA032573*, Natl. Tech. Inf. Serv., Springfield, VA.

Thomson, N. R. (1993), Experimental daytime VLF ionospheric parameters, *J. Atmos. Terr. Phys.*, *55*, 173-184.

Thomson, N.R. (2010), Daytime tropical D-region parameters from short path VLF phase and amplitude, *J. Geophys. Res.*, *115*, A09313, doi:10.1029/2010JA015355.

Thomson, N. R. and M. A. Clilverd (2001), Solar flare induced ionospheric D-region enhancements from VLF amplitude observations. *J. Atmos. Sol-Terr. Phys.*, *63*(16), 1729-1737.

Thomson, N.R., M. A. Clilverd and C. J. Rodger (2011a), Daytime midlatitude D-region parameters at solar minimum from short-path VLF phase and amplitude, *J. Geophys. Res.*, *116*, A03310, doi:10.1029/2010JA016248.

Thomson, N.R., C. J. Rodger and M. A. Clilverd (2011b), Daytime D-region parameters from long-path VLF phase and amplitude, *J. Geophys. Res.*, *116*, A11305, doi:10.1029/2011JA016910.

Thomson, N.R., C. J. Rodger and M. A. Clilverd (2012), Tropical daytime lower D-region dependence on sunspot number, *J. Geophys. Res.*, *117*, A10306, doi:10.1029/2012JA018077.

Vincenty, T. (1975), Direct and inverse solutions of geodesics on the ellipsoid with application of nested equations, *Survey Review*, *23(*176), 88-93.

Wait, J.R., and K.P. Spies (1964), Characteristics of the Earth-ionosphere waveguide for VLF radio waves. *NBS Tech. Note 300*, Natl. Bur. of Stand., Boulder, Colo.

Yoshida, M., T. Yamauchi, T. Horie, and M. Hayakawa (2008), On the generation mechanism of terminator times in subionospheric VLF/LF propagation and its possible application to seismogenic effects, *Natural Hazards Earth System Sci., 8,* 129-134.

Table

Table 1. Calculated Kauai-Keauhou Free-Space Delay Differences[a]

Locations/Paths	Latitude (deg)	Longitude (°E.)	Dist. (km)	Delay (μs)
NPM	21.4202	-158.1511		
Keauhou Beach Resort	19.5765	-155.9680	305.81	1020.1
Lydgate Park, Kauai	22.0385	-159.3362	140.42	468.4
Δf: Keauhou – Lydgate			165.39	551.7
Δf: modulo half cycle				14.3

[a]Rows 1–4 show the locations/paths with calculated distances and free space delays for NPM-Keauhou, NPM-Lydgate and Lydgate-Keauhou. Row 5 then shows the Lydgate-Keauhou free-space delay difference modulo half a cycle of 21.4 kHz.

Figure Captions

Figure 1. The 306-km path (red) used to determine tropical D-region values of *H'* and β as functions of solar zenith angle. The shorter 140-km path (blue) enabled the phase and power of the transmitter itself to be determined.

Figure 2. Phases and amplitudes of NPM recorded at Forks WA near Seattle, while NPM portable loop measurements were being made in Hawaii. (02 UT on 21 Aug 2012 UT is shown as 26 UT on 20 Aug 2012 UT etc. to give convenient plot continuity across the UT date change near path midday.)

Figure 3. Calculated phases and amplitudes for NPM (21.4 kHz) to Keauhou (306 km) as functions of *H'* and β. Also shown are the observed midday phase and amplitude which thus give *H'* = 69.3 km and β = 0.49 km^{-1} for midday.

The larger open circles (blue for morning and purple for afternoon) show representative points plotted from Figure 4 and used in Figure 5, as explained in the text.

Figure 4. Observed phases and amplitudes (dB > 1 μV/m) of NPM at Keauhou, Big Island, Hawaii, 19-25 August 2012. The vertical dashed lines show midday local time. (As in Figure 2, 02 UT on 21 Aug is shown as 26 UT on 20 Aug etc.)

Figure 5. Observed height, *H'*, in km, and sharpness, β, in km^{-1} versus solar zenith angle for the tropical short paths, NPM to Keauhou (August, 2012) and NWC to Karratha (October, 2011).). **The blue crosses and dashed lines are the reflections about noon of the (black) NPM afternoon data to allow comparison with morning data as discussed in the text.**

Figure 6. Observed height *H'*, in km, and sharpness β, in km^{-1}, versus solar zenith angle for the low latitude short path NPM to Keauhou (August 2012) compared with the mainly low latitude, trans-equatorial, long path NWC, N.W. Australia, to Kyoto, Japan (August 1968).

Figure 7. Observed *H'* and β versus solar zenith angle for the low to mid-latitude path from NAU, Puerto Rico, to St. John's NL Canada (June 2013) compared with *H'* and β from the NPM-Keauhou short, low latitude path.

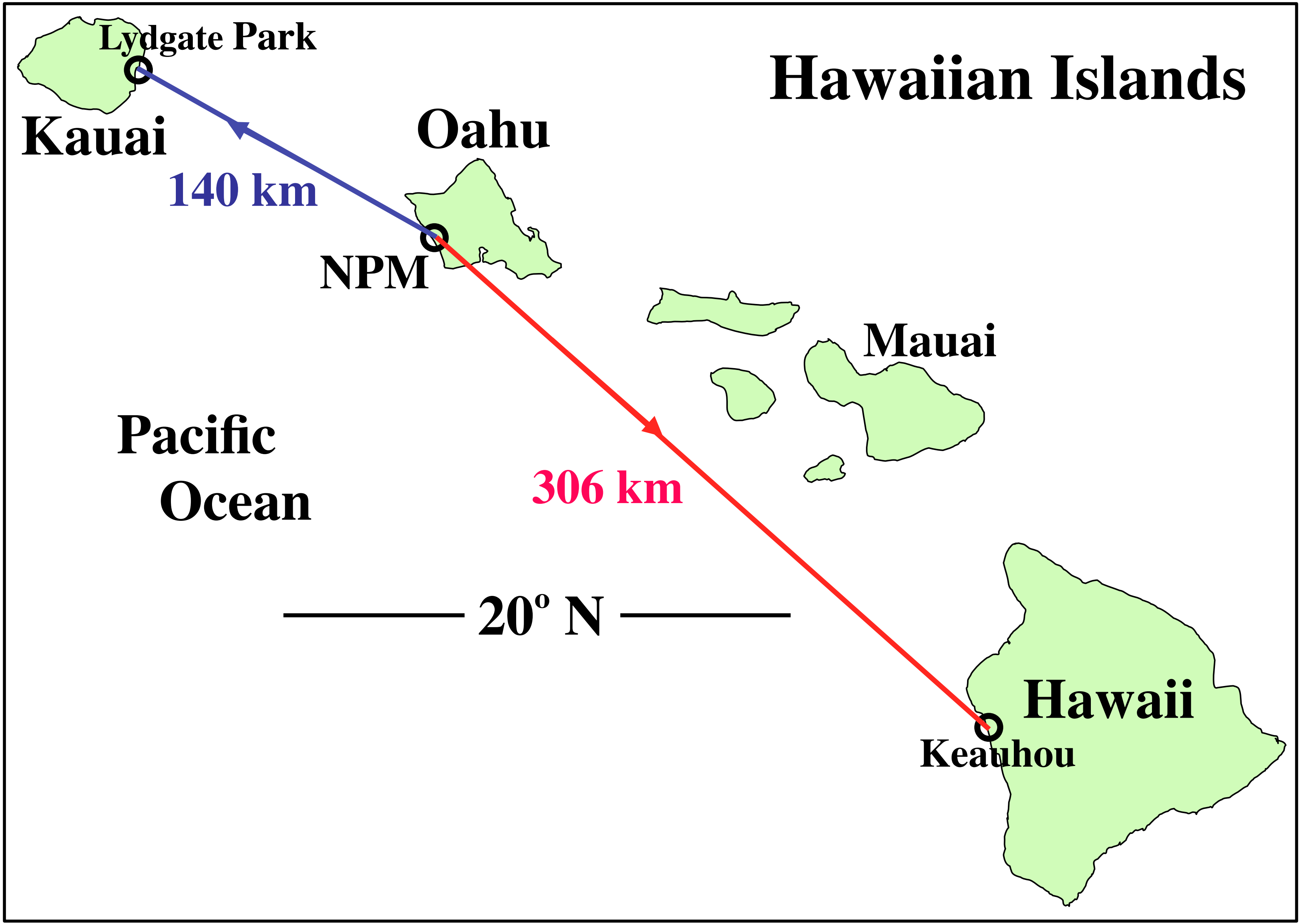
Hawaiian Islands
Lydgate Park
Kauai
Oahu
140 km
NPM
Mauai
Pacific Ocean
306 km
20° N
Hawaii
Keauhou

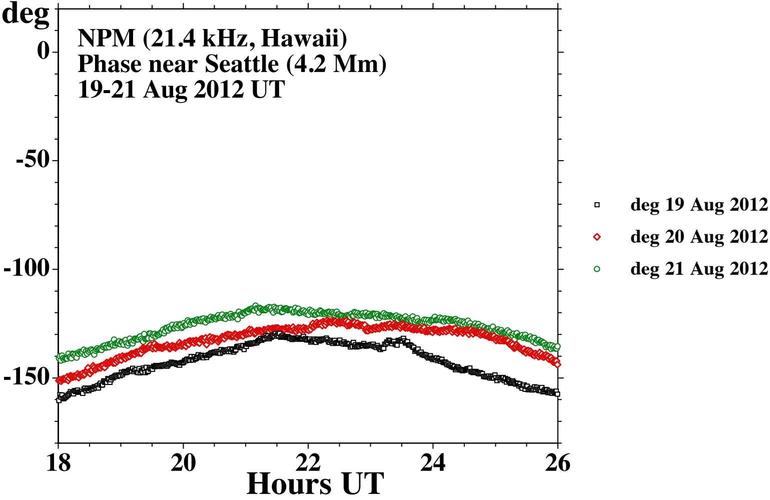
deg
NPM (21.4 kHz, Hawaii)
Phase near Seattle (4.2 Mm)
19-21 Aug 2012 UT
0
-50
-100
-150
18
20
22
24
26
Hours UT
deg 19 Aug 2012
deg 20 Aug 2012
deg 21 Aug 2012

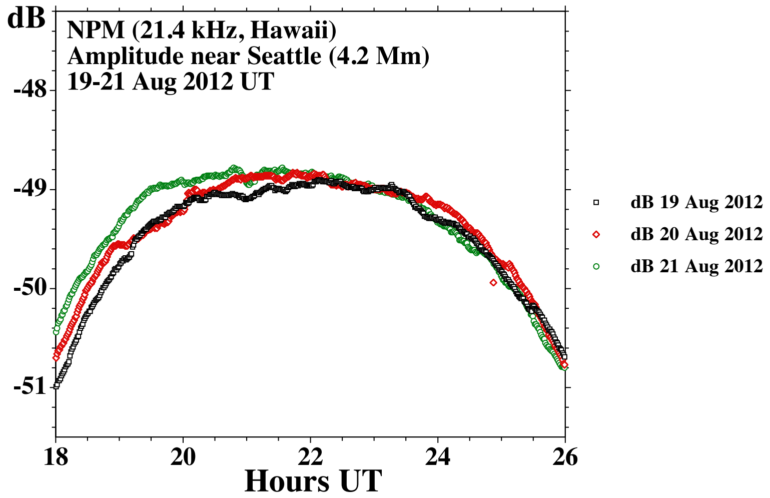
dB
NPM (21.4 kHz, Hawaii)
Amplitude near Seattle (4.2 Mm)
19-21 Aug 2012 UT
-48
-49
-50
-51
18
20
22
24
26
Hours UT
dB 19 Aug 2012
dB 20 Aug 2012
dB 21 Aug 2012

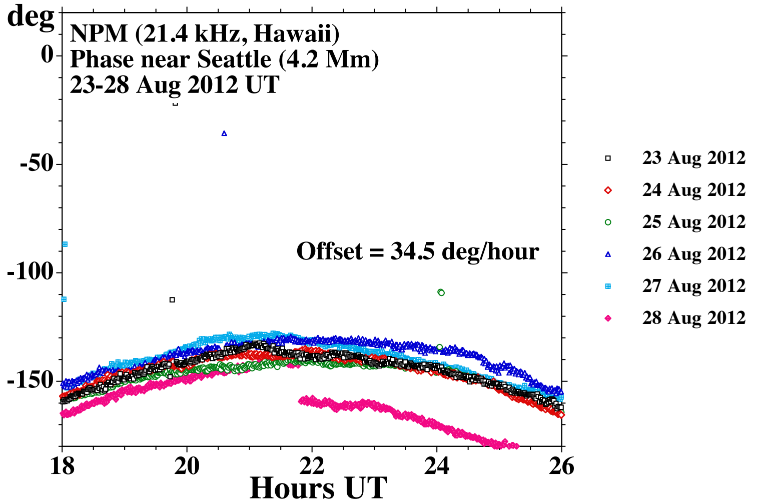
deg
NPM (21.4 kHz, Hawaii)
Phase near Seattle (4.2 Mm)
23-28 Aug 2012 UT
0
-50
-100
-150
Offset = 34.5 deg/hour
18
20
22
24
26
Hours UT
23 Aug 2012
24 Aug 2012
25 Aug 2012
26 Aug 2012
27 Aug 2012
28 Aug 2012

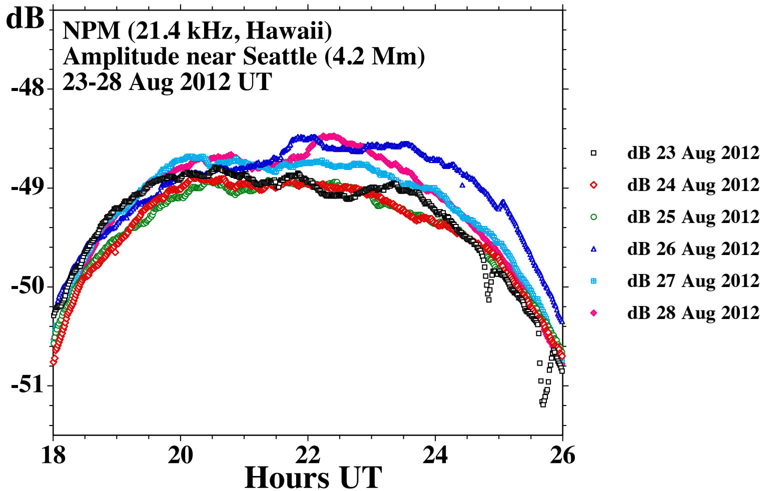
dB
NPM (21.4 kHz, Hawaii)
Amplitude near Seattle (4.2 Mm)
23-28 Aug 2012 UT
-48
-49
-50
-51
18
20
22
24
26
Hours UT
dB 23 Aug 2012
dB 24 Aug 2012
dB 25 Aug 2012
dB 26 Aug 2012
dB 27 Aug 2012
dB 28 Aug 2012

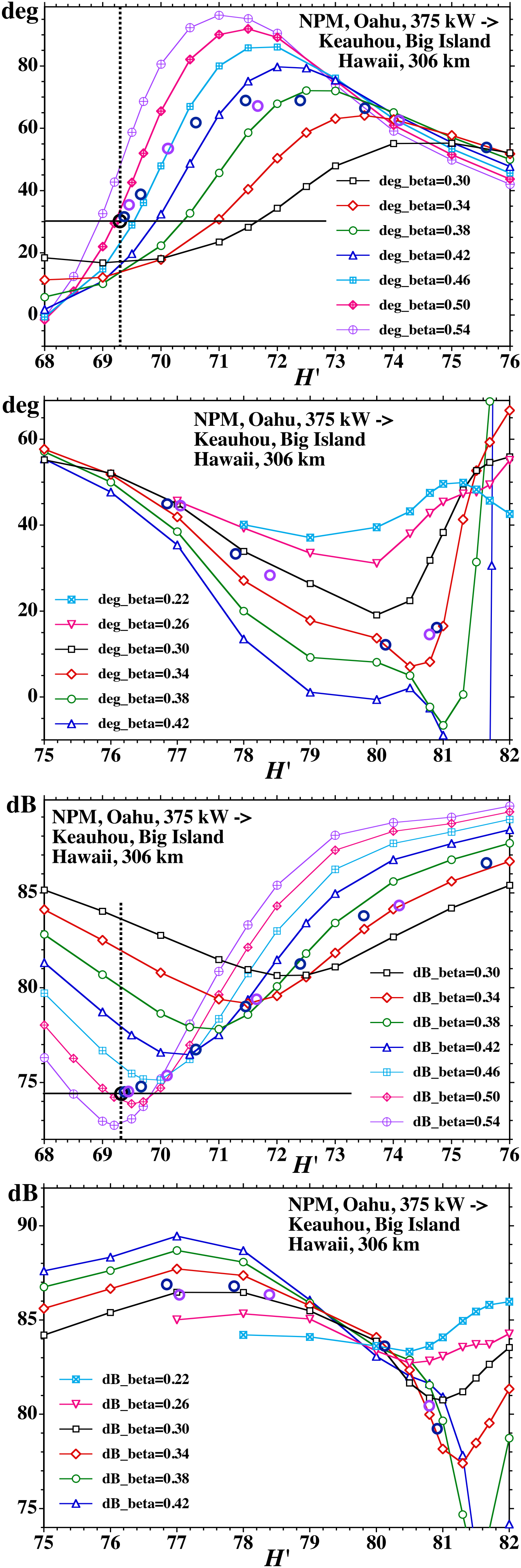

deg
NPM, Oahu, 375 kW ->
Keauhou, Big Island
Hawaii, 306 km
deg_beta=0.30
deg_beta=0.34
deg_beta=0.38
deg_beta=0.42
deg_beta=0.46
deg_beta=0.50
deg_beta=0.54
H'
deg
NPM, Oahu, 375 kW ->
Keauhou, Big Island
Hawaii, 306 km
deg_beta=0.22
deg_beta=0.26
deg_beta=0.30
deg_beta=0.34
deg_beta=0.38
deg_beta=0.42
H'
dB
NPM, Oahu, 375 kW ->
Keauhou, Big Island
Hawaii, 306 km
dB_beta=0.30
dB_beta=0.34
dB_beta=0.38
dB_beta=0.42
dB_beta=0.46
dB_beta=0.50
dB_beta=0.54
H'
dB
NPM, Oahu, 375 kW ->
Keauhou, Big Island
Hawaii, 306 km
dB_beta=0.22
dB_beta=0.26
dB_beta=0.30
dB_beta=0.34
dB_beta=0.38
dB_beta=0.42
H'

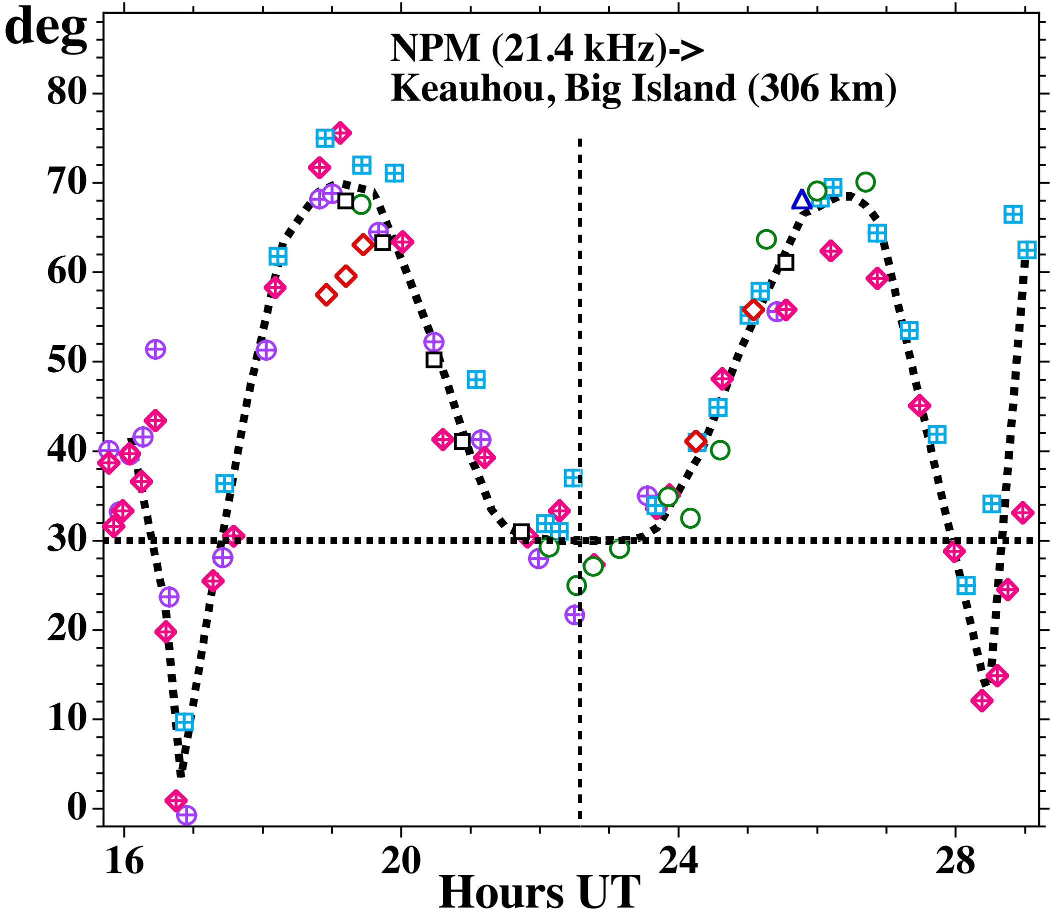

deg
NPM (21.4 kHz)->
Keauhou, Big Island (306 km)
80
70
60
50
40
30
20
10
0
16
20
24
28
Hours UT

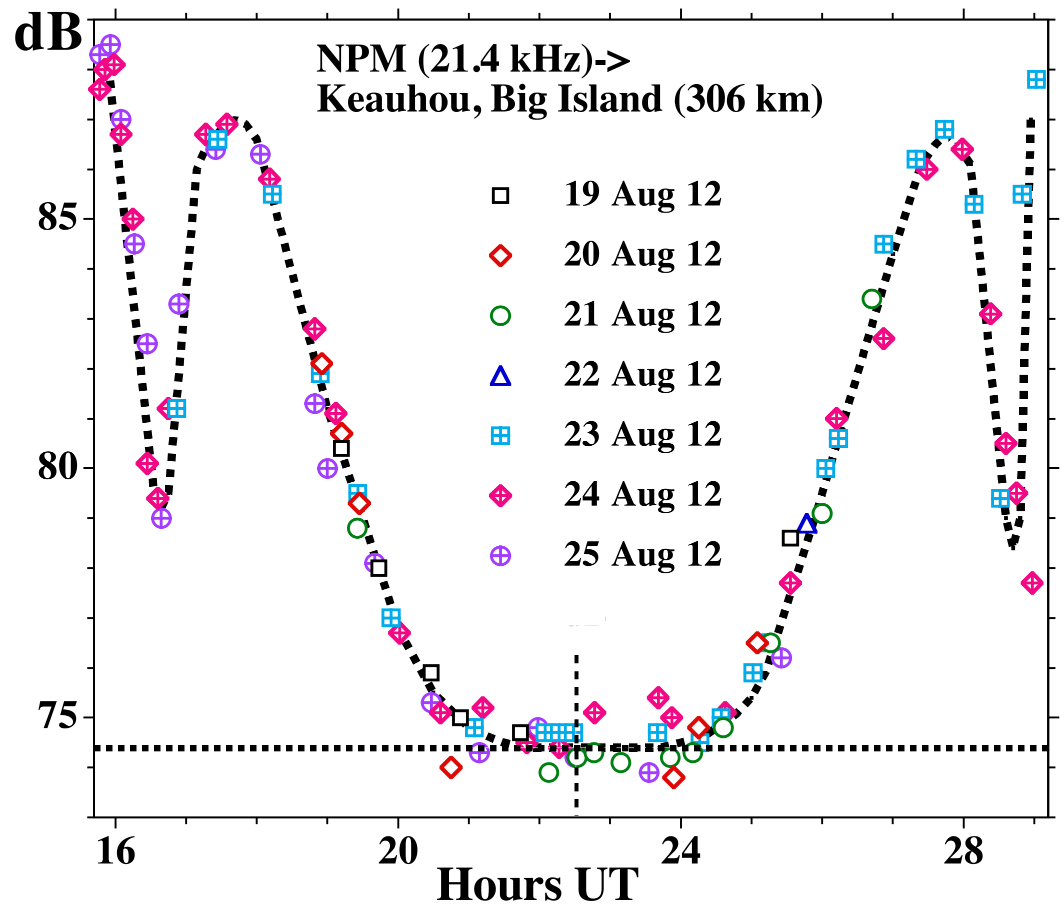

dB
NPM (21.4 kHz)->
Keauhou, Big Island (306 km)
19 Aug 12
20 Aug 12
21 Aug 12
22 Aug 12
23 Aug 12
24 Aug 12
25 Aug 12
85
80
75
16
20
24
28
Hours UT

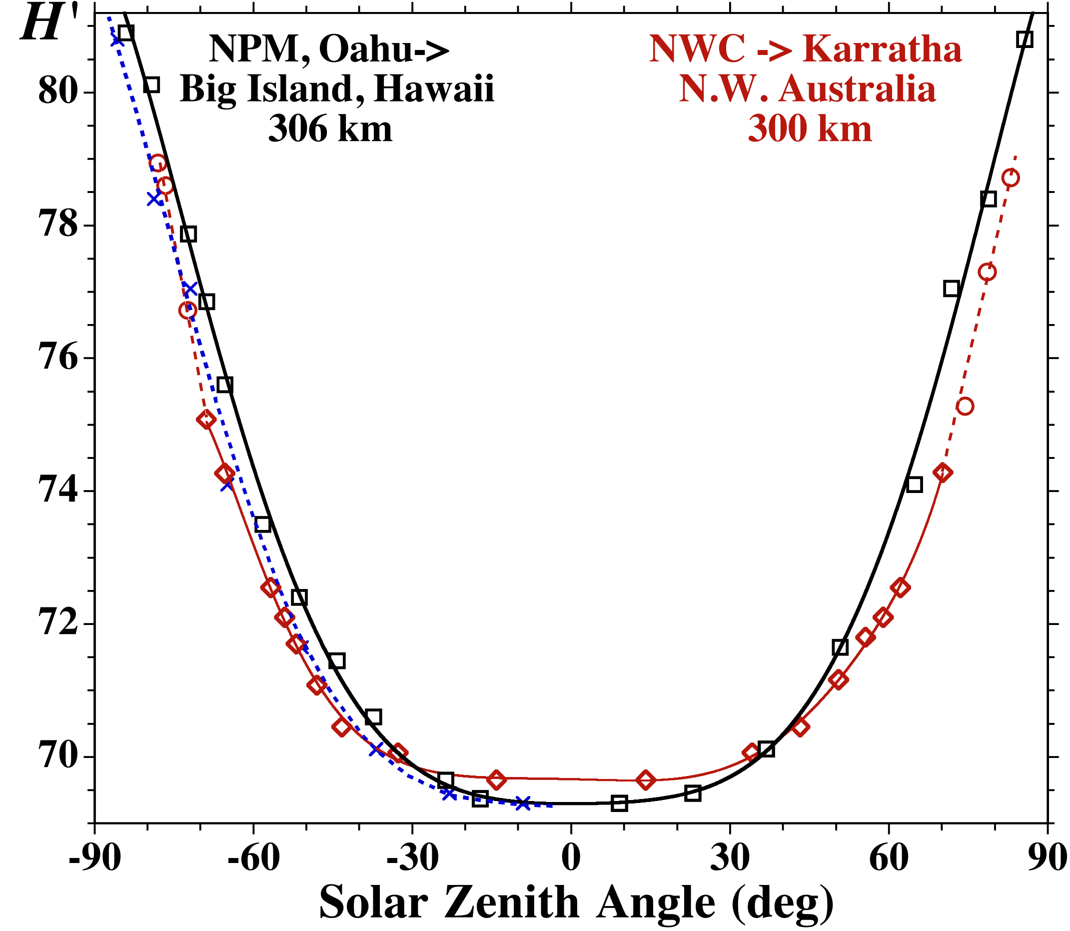
H'
NPM, Oahu->
Big Island, Hawaii
306 km
NWC -> Karratha
N.W. Australia
300 km
80
78
76
74
72
70
-90
-60
-30
0
30
60
90
Solar Zenith Angle (deg)

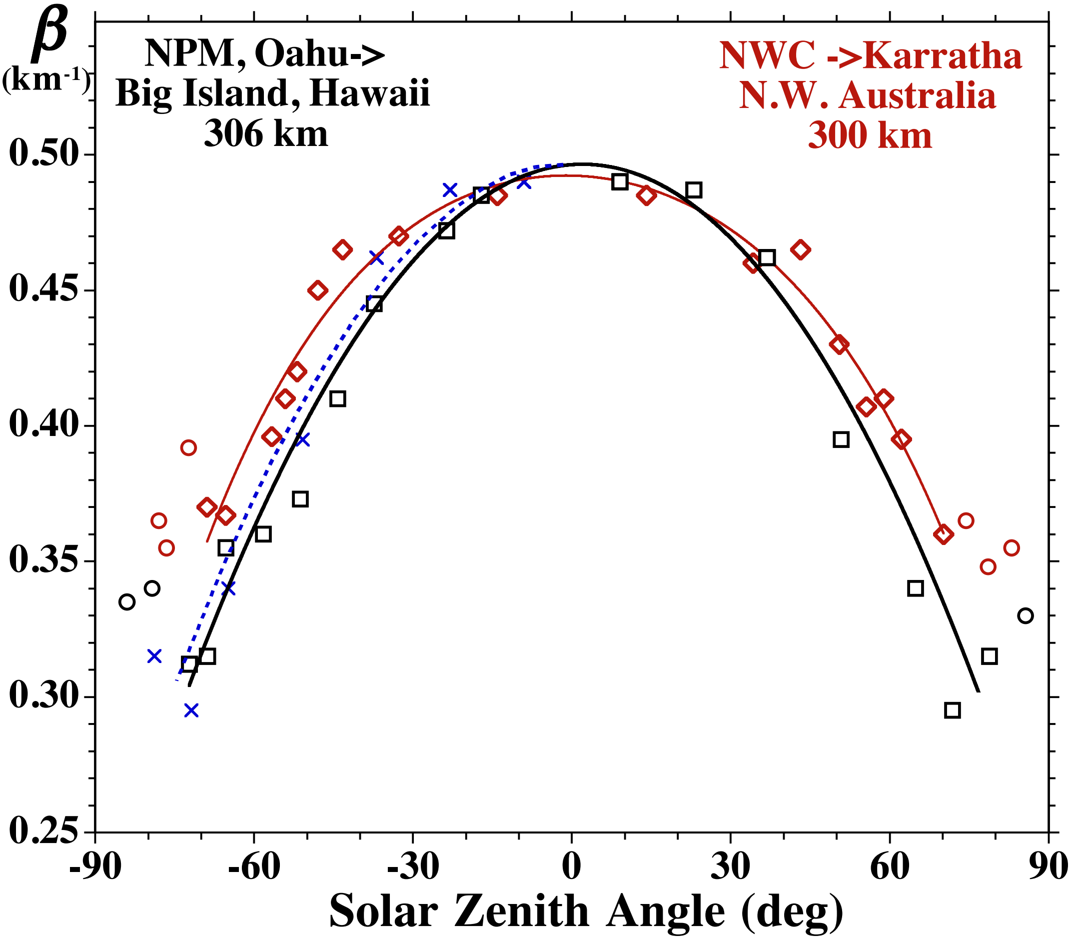
β
(km⁻¹)
NPM, Oahu->
Big Island, Hawaii
306 km
NWC ->Karratha
N.W. Australia
300 km
0.50
0.45
0.40
0.35
0.30
0.25
-90
-60
-30
0
30
60
90
Solar Zenith Angle (deg)

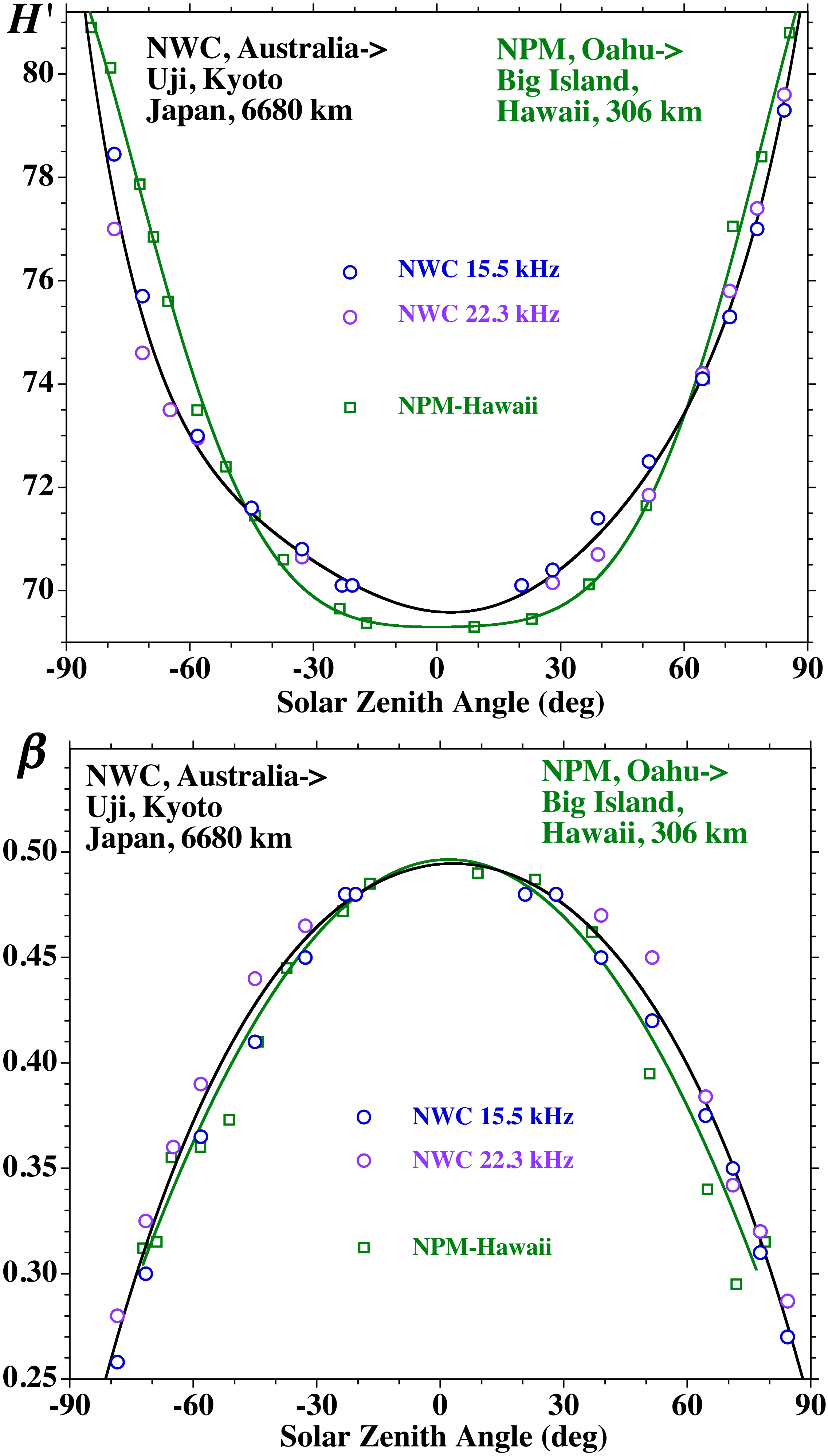

H'
NWC, Australia->
Uji, Kyoto
Japan, 6680 km
NPM, Oahu->
Big Island,
Hawaii, 306 km
NWC 15.5 kHz
NWC 22.3 kHz
NPM-Hawaii
80
78
76
74
72
70
-90
-60
-30
0
30
60
90
Solar Zenith Angle (deg)
β
NWC, Australia->
Uji, Kyoto
Japan, 6680 km
NPM, Oahu->
Big Island,
Hawaii, 306 km
NWC 15.5 kHz
NWC 22.3 kHz
NPM-Hawaii
0.50
0.45
0.40
0.35
0.30
0.25
-90
-60
-30
0
30
60
90
Solar Zenith Angle (deg)

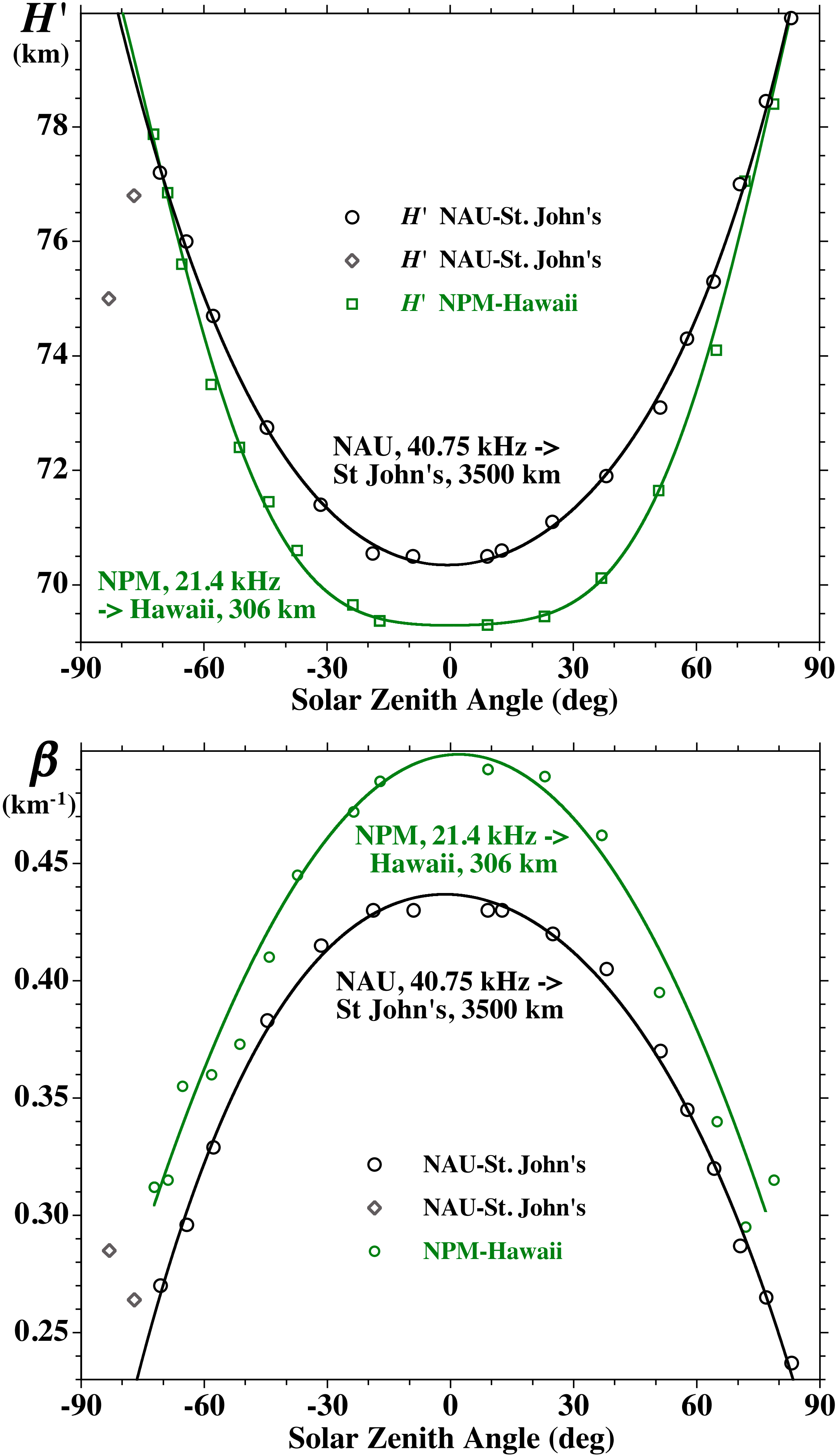

H'
(km)
78
76
74
72
70
H' NAU-St. John's
H' NAU-St. John's
H' NPM-Hawaii
NAU, 40.75 kHz ->
St John's, 3500 km
NPM, 21.4 kHz
-> Hawaii, 306 km
-90
-60
-30
0
30
60
90
Solar Zenith Angle (deg)
β
(km-1)
0.45
0.40
0.35
0.30
0.25
NPM, 21.4 kHz ->
Hawaii, 306 km
NAU, 40.75 kHz ->
St John's, 3500 km
NAU-St. John's
NAU-St. John's
NPM-Hawaii
-90
-60
-30
0
30
60
90
Solar Zenith Angle (deg)